



## Potential dissolution and photo-dissolution of ZnO thin films

Jie Han, Wei Qiu, Wei Gao\*

Department of Chemical & Materials Engineering, The University of Auckland, 20 Symonds Street, Auckland 1010, New Zealand

### ARTICLE INFO

#### Article history:

Received 25 August 2009

Received in revised form

12 November 2009

Accepted 12 January 2010

Available online 18 January 2010

#### Keywords:

Zinc oxide

Photocatalyst

Dissolution

Photo-dissolution

### ABSTRACT

Potential dissolution and photo-dissolution are important concerns for zinc oxide (ZnO) photocatalysts due to the possible results of catalyst inactivation and secondary pollution from free  $Zn^{2+}$ . In this study, magnetron-sputtered ZnO thin films were prepared and exposed under a series of corrosive conditions. ZnO films suffered rapid dissolution under: (a) extreme pH levels ( $\leq 5$  or  $\geq 11$ ); (b) 1 mM ethylenediaminetetraacetic acid (EDTA) solution; (c) UV ( $\lambda = 254$  nm). The dissolution rate of ZnO films was moderate at pH = 6 and decreased markedly as pH increased to 7. It continued to decrease as pH increased from 7 to 10, then the trend quickly reversed as pH increased further. The lowest dissolution rate was obtained at pH = 10, with only 1.2% ZnO dissolved after 24 h of exposure. Minimal dissolution was observed on ZnO films in alkalised 1 mM oxalate and acetate solutions. Pitting corrosion was observed on ZnO films after UV irradiation, which was ascribed to photo-generated holes on surface defect sites. The presence of hole scavengers ( $Na_2SO_3$ ) caused significant suppression on ZnO photo-dissolution. This suppression effect remained in place until hole scavengers were completely consumed, from where the photo-dissolution rates accelerated.

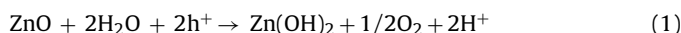
© 2010 Elsevier B.V. All rights reserved.

### 1. Introduction

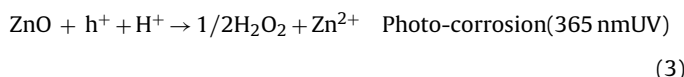
Zinc oxide (ZnO) has been extensively studied as a photocatalyst and a potential material to fabricate self-cleaning surfaces, often in parallel with the benchmark photocatalyst titanium dioxide ( $TiO_2$ ). Although  $TiO_2$  is generally recognised as the most suitable photocatalyst, ZnO differentiates itself by several interesting properties, i.e. visible-light-responsive photocatalytic activity [1], stable photocatalytic activity at high temperature (873 K) [2], higher  $H_2O_2$  generation rate in water under UV [3], and ease of doping [4–8]. It has also been reported that ZnO exhibited higher activity than  $TiO_2$  in the photocatalytic degradation of specific dyes [9–11]. In its nano-structured form, ZnO thin films showed switchable surface wettability, i.e. surface transforms reversibly from highly hydrophobic in dark to superhydrophilic under UV [12–14]. Nano-structured ZnO films have shown superior surface hydrophobicity than  $TiO_2$ , which makes them an attractive alternative to fabricate self-cleaning surfaces such as self-cleaning glasses and building coatings [15–18]. In these potential applications, the stability of ZnO is vital as ZnO is likely to be exposed in corrosive environments.

Early studies have found that ZnO could be corroded under electrochemical conditions, in acids and under UV. Rao et al. [19] reported a gradual decay of  $H_2$  production in a UV-irradiated ZnO/water suspension. Although not unequivocally proved, the

authors suspected that the decay was due to ZnO photo-dissolution under UV, as intense bands corresponding to  $OH^-$  were observed in the infrared spectrum of used ZnO. The following reaction was suggested:



Fruhwith et al. [20] developed an electrochemical model for the linear pH dependence of flat-band potential and ZnO dissolution rates. The following reactions were suggested:



Spathis and Poullos [21] further examined the corrosion of Zn and ZnO coatings by weight loss and potentiodynamic anodic polarization. The authors found the main corrosion products being  $Zn(OH)_2$  and zinc oxychlorides under dark and UV illumination, respectively. Furthermore, Futsuhara et al. [22] developed a method to create micro-patterns on ZnO films by corroding ZnO films with a bias voltage under high pH levels and UV irradiation ( $40$  mW/cm<sup>2</sup>).

Several recent studies have reported activity deterioration of ZnO photocatalysts. Such results were often ascribed to the dissolution or photo-dissolution of ZnO; however, limited experimental evidence was presented or sought. In a photocatalytic degrada-

\* Corresponding author. Tel.: +64 9 373 7999x88175; fax: +64 9 373 7463.

E-mail address: [w.gao@auckland.ac.nz](mailto:w.gao@auckland.ac.nz) (W. Gao).

tion study of polyvinylchloride, Hidaka et al. [23] reported that ZnO showed a higher initial dechlorination rate than TiO<sub>2</sub> but soon suffered activity deterioration. Neppolian et al. [24] observed the inactivation of ZnO photocatalysts, and suggested that this should be due to the incongruous dissolution yielding Zn(OH)<sub>2</sub> on ZnO surface as well as photo-dissolution of ZnO by self-oxidation. Several studies have given evidences of ZnO dissolution and photo-dissolution, but the effects of experimental conditions on the occurrence and extent of ZnO dissolution and photo-dissolution were not well understood. For instance, Lathasree et al. [25] tested the reusability of ZnO photocatalysts and found that a small extent (0.04%) of ZnO had undertaken photo-dissolution after 2 h of reaction. Yassitepe et al. [26] reported that the photocatalytic activity of ZnO plates gradually decreased but the activity was recovered by stored in dark overnight. Furthermore, Wang et al. [27] embedded ZnO nanoparticles in Nafion membranes and found ZnO particles being highly stable with hardly any reduction of activity after 10 times of repeated reaction cycles.

In this study, the dissolution and photo-dissolution behaviour of ZnO thin films is investigated under a series of corrosive conditions. Our study aims to conduct a systematic study to identify the occurrence, assess the extent, and understand the causes and reaction mechanisms of ZnO dissolution and photo-dissolution. The chemical dissolution of ZnO was studied by exposing ZnO films to a wide range of pH levels (3–12) and three alkalis ligand solutions, i.e. EDTA, oxalic acid and acetic acid. The photo-dissolution of ZnO was examined by exposing ZnO films under UV with different irradiation intensities. The effect of hole scavengers (Na<sub>2</sub>SO<sub>3</sub>) on ZnO photo-dissolution was also studied and discussed.

## 2. Experimental

### 2.1. Preparation

ZnO thin films were prepared by magnetron sputtering. Microscope slides (75 mm × 25 mm × 1 mm) were rinsed in deionised water, ultrasonically cleaned in ethanol and dried before used as substrates. The cleaned slides were put into a working chamber which had been vacuumed to  $2 \times 10^{-6}$  Torr and cleaned by a radio frequency (rf) plasma for 1 h before argon was introduced. Sputtering was conducted with a dc power of 0.25A for the direct deposition from a ZnO target (99.99% purity, Beijing Mountain Tech). The sputtering process was continued for 30 min to obtain ZnO thin films with an approximate thickness of 150 nm.

### 2.2. Chemical dissolution

#### 2.2.1. Dissolution in acid and alkali solutions

A series of water solutions with initial pH levels from 3 to 12 were used to investigate the influence of pH on ZnO dissolution. Initial pH levels were adjusted by adding HCl acid (Analytical Grade, BDH Chemicals, UK) and NaOH (Analytical Grade, Ajax FineChem, New Zealand). The pH levels were measured on a pH meter with two-decimal-place accuracy (CyberScan 510, Eutech). In each experiment, a ZnO film was immersed in 500 ml solution with a designated pH level between 3 and 12. At certain time intervals, 5 ml samples were taken from the solution and filtered through a 0.45 μm syringe filter (BioLab, New Zealand). The concentration of dissolved Zn<sup>2+</sup> in each sample was measured by Atomic Absorption Spectroscopy (AAS, Varian SpectrAA 50). After the reaction, the solution was acidified and stirred to completely dissolve the remained ZnO film on glass substrate. The original amount of ZnO film was calculated by measuring the Zn<sup>2+</sup> concentration in the final solution as well as the samples taken from the solution during the reaction.

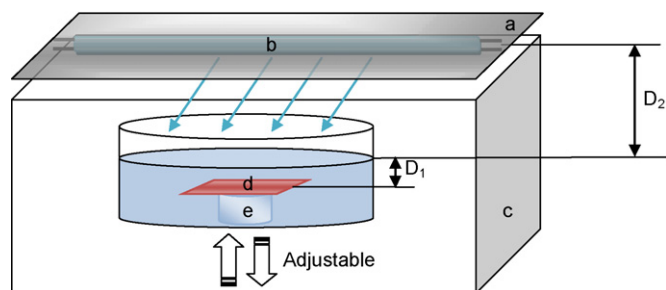


Fig. 1. Experiment set-up for ZnO photo-dissolution study: (a) lid; (b) UV lamp; (c) safety enclosure; (d) ZnO film on a microscope slide; (e) support.

#### 2.2.2. Dissolution in ligand solutions

EDTA (Analytical Grade, BDH Chemicals, UK), oxalic acid (Reagent Grade, 99.5%, Scharlau Chemie S.A., Spain) and acetic acid (ACS Reagent Grade, Scharlau Chemie S.A., Spain) were used to investigate potential dissolution of ZnO by forming complexes with these ligands. Each ligand was dissolved in deionised water to prepare 500 ml of 1 mM ligand solution. The initial pH was adjusted to 10 to minimise the influence of pH on ZnO dissolution therefore the sole effect of ligand-assisted dissolution can be measured. Oxalic acid and acetic acid quickly dissolved in water, while the dissolution of EDTA solids was slow prior to the pH adjustment. After the pH adjustment, EDTA solids completely dissolved after 30 min continuous stirring. A prepared ZnO film was immersed in each ligand solution for 24 h. Samples were taken from the solution during the reaction and filtered before AAS measurements.

### 2.3. Photo-dissolution

#### 2.3.1. Photo-dissolution without hole scavengers

The photo-dissolution of ZnO films was studied using the apparatus in Fig. 1. A 22 W UV lamp (254 nm, Contamination Control, New Zealand) was used as UV source. ZnO films were immersed in water and exposed under UV for 24 h. The distance from the ZnO film to the water surface (D<sub>1</sub> in Fig. 1) was fixed at 1.3 cm in all experiments to maintain a consistent attenuation factor for the incident UV. To investigate the effect of UV intensity, the distance between the UV lamp and water surface (D<sub>2</sub> in Fig. 1) was adjusted to 2.4, 4.8 and 7.2 cm, respectively. The incident UV intensity on the water surface was measured by a radiometer (IL1700, International Light, USA). A blank experiment without UV irradiation was conducted as a reference.

#### 2.3.2. Photo-dissolution with hole scavengers

The influence of hole scavengers on ZnO photo-dissolution was studied by immersing ZnO thin films under UV in a 10 mM and 100 mM Na<sub>2</sub>SO<sub>3</sub> (Analytical Grade, BDH Chemicals, UK) solution, respectively. The apparatus in Fig. 1 was used and the distance between the UV lamp and water surface (D<sub>2</sub>) was fixed at 2.4 cm. The initial pH level of the 10 mM and 100 mM Na<sub>2</sub>SO<sub>3</sub> solutions was 8.2 and 8.5, respectively.

### 2.4. Characterisation

The prepared ZnO thin films were characterised by X-ray diffraction (XRD). Light transmittance of the ZnO-coated microscope slides was measured on a UV–vis spectrometer (Agilent 8453) using a blank, clean microscope slide as reference. Scanning Electron Microscope with Energy Dispersive X-ray Spectrometer (SEM-EDS, Philips XL30S FEG) was used to examine the morphology and surface composition of ZnO films before and after exposure in corrosive conditions for 6 h. The used ZnO films were gently rinsed by deionised water and dried at 60 °C overnight prior to SEM

characterisation. To ensure the ZnO films remained on substrates were thick enough for EDS testing, special ZnO films were used with 500-nm thicknesses. The special ZnO films were exposed in the same corrosive condition as 150-nm-thick ZnO film samples for 3 h.

### 3. Results and discussions

#### 3.1. Characterisation of ZnO films

A typical surface morphology of the prepared ZnO film is shown in Fig. 2. It is shown that a uniform and compact layer of ZnO thin film was deposited on the substrate after 30-min magnetron sputtering. As shown in Fig. 2(a), the nanograins are rather uniform in sizes (30–50 nm) and compactly stacked, forming a ‘flat’ and compact surface structure. It is expected that such compact surface structure will have more resistance to corrosive substances, compared to the ZnO films prepared by anodizing which consisted of a thin compact inner layer and an outer porous layer [21]. The cross-section SEM image in Fig. 2(b) shows that the thickness of the ZnO film is in the range of 135–150 nm.

The XRD pattern of the ZnO thin film is shown in Fig. 3. It is known that the sputtered ZnO films are textured, with *c*-axis lies perpendicular to the substrate surface [28]. In Fig. 3, the ZnO thin film shows a single peak at the scattering angle ( $2\theta$ ) of  $34.2^\circ$ , which corresponds to the X-ray diffraction from the 002 crystal plane (JCPDS No. 80-0075). The average size

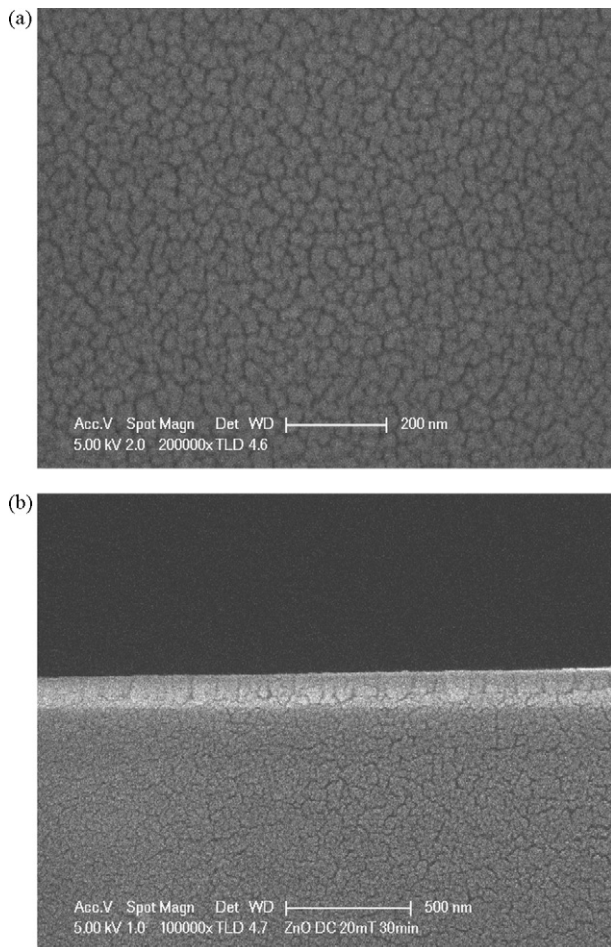


Fig. 2. Surface and cross-section morphology of the prepared ZnO film.

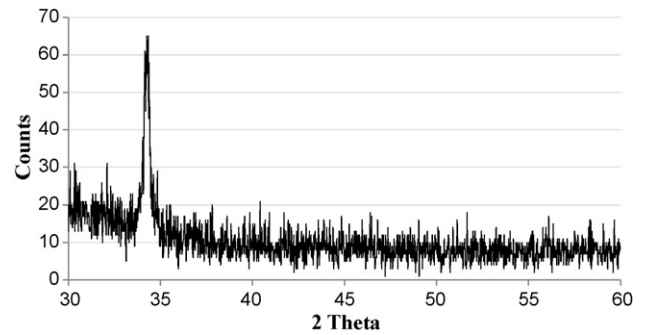


Fig. 3. X-ray diffraction spectrum of the prepared ZnO film.

of ZnO nanograins can be estimated by the Debye–Scherrer formula:

$$\tau = \frac{K\lambda}{\beta \cos \theta} \quad (4)$$

where  $\tau$  is the mean size of the ordered (crystalline) domains,  $K$  is the shape factor,  $\lambda$  is the X-ray wavelength, and  $\beta$  is the line broadening at half the maximum intensity (FWHM) on the  $2\theta$  scale, and  $\theta$  is the Bragg angle of the peak. The average crystal size in ZnO films was calculated as 16.4 nm, which is smaller than the grain size (30–50 nm) estimated from Fig. 2(a).

Light transmittance is an important property for ZnO thin films given their potential uses on self-cleaning glasses. It is shown in Fig. 4 that the prepared ZnO thin film has high light transmittance (80–91%) to visible light (400–750 nm). It is expected that the flat and compact surface structure contributed to the high light transmittance as light transmittance is largely affected by the extent of light scattering which, in turn, is determined by surface roughness and film porosity. It is also worthwhile to note that the prepared ZnO thin films are relatively thick (150 nm), comparing to the commercial Pilkington Activ™ self-cleaning glass which has a 25-nm-thick  $\text{TiO}_2$  film coated on glass [17]. The high visible-light transmittance indicates that ZnO thin films are likely to meet the aesthetic requirements for coatings on glass buildings. Moreover, the high transmittance (>90%) for infrared spectrum (>750 nm) shows that infrared light in solar irradiation can easily go through the ZnO film, while the sharp decrease of transmittance for UV (<400 nm) indicates efficient absorption of UV by the ZnO film. Both are favourable features from the prospective of sustainable building design.

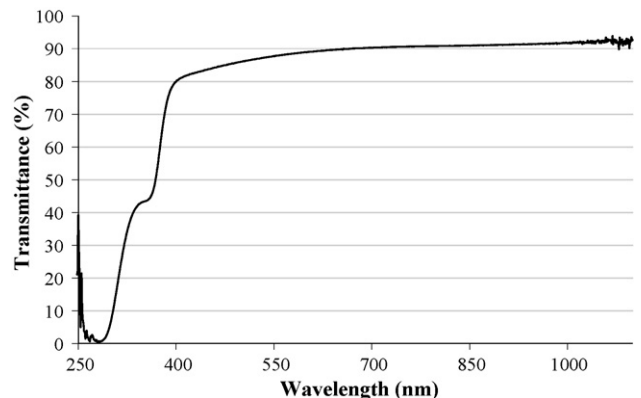


Fig. 4. Light transmittance of the prepared ZnO film.

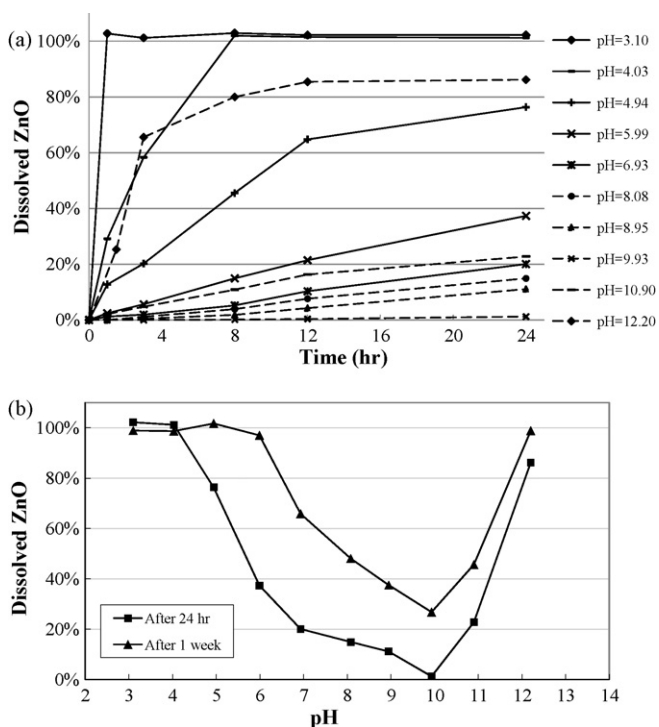


Fig. 5. Dissolution of ZnO films in aqueous solutions at different pH level: (a) within 24 h; (b) after 24 h and 1 week.

### 3.2. Chemical dissolution

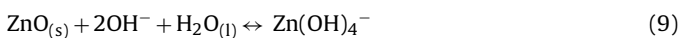
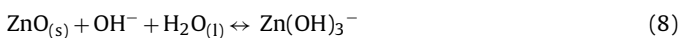
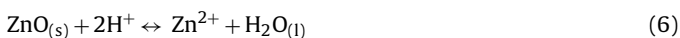
#### 3.2.1. Dissolution in acid and alkaline solutions

As shown in Fig. 5, pH level has a significant influence on the ZnO dissolution. At pH = 3.1, the ZnO film completely dissolved within 1 h, while at pH = 4.0 the dissolution was completed in 8 h. The percentage of dissolved ZnO ( $ZnO_{(d)}\%$ ), dropped significantly as pH increased to 4.9 and 6.0, indicating the negative effect of weaker acidity. As pH increased further,  $ZnO_{(d)}\%$  continued to drop and reached the lowest at pH = 9.9. The trend then quickly reversed as pH increasing to 10.9 and 12.2, with  $ZnO_{(d)}\%$  increased considerably as shown in Fig. 5(a). This trend reversal is more evident in Fig. 2(b), where  $ZnO_{(d)}\%$  is plotted against pH after 24 h and 1 week of exposure.

The solubility of a metal oxide in aqueous solution without the presence of metal-complexing ligands can be generally expressed as:

$$\sum Me_T = [Me^{z+}] + \sum_{i=1}^n [Me(OH)_i^{z-i}] \quad (5)$$

where  $Me^{z+}$  represents the metal cation;  $z$  is the valence of metal cation;  $Me(OH)_i^{z-i}$  is the hydroxide complex. The following reactions were suggested for ZnO in water [29]:



Another reaction is also possible however the solubility of the product is minimal in water.



Table 1

Surface composition of ZnO films (500-nm thick) before and after 24 h of exposure at various pH.

	Composition (atom%)		
	Zn	O	Zn/O ratio
Before exposure	64.14	35.86	1.789
After exposure (pH = 4.0)	64.20	35.80	1.794
After exposure (pH = 6.1)	64.47	35.53	1.815
After exposure (pH = 8.1)	64.17	35.83	1.791
After exposure (pH = 10.1)	63.64	36.36	1.750
After exposure (pH = 12.0)	64.35	35.65	1.805

In terms of Eqs. (6)–(9), the total concentration of dissolved ZnO is

$$\sum Zn_T = [Zn^{2+}] + [ZnOH^+] + [Zn(OH)_3^-] + [Zn(OH)_4^{2-}] \quad (11)$$

Depending on the pH of the solution, one or more reactions may be predominant. In highly acidic solutions, the dissolution of ZnO is more likely to be the result of direct proton attacks on surface Zn–O bonds, followed by the dissociation of Zn (Eqs. (6) and (7)). If pH increases and solution becomes near neutral,  $H^+$  becomes rare which lowers the frequency of proton attacks. This is evidenced by our results in Fig. 5(a).

Eqs. (8) and (9) suggest that ZnO could also dissolve in alkaline solutions by forming hydroxo complexes with  $OH^-$ . It is therefore expected that the change from neutral to weak alkaline solution may re-accelerate ZnO dissolution by having more  $OH^-$  ions available. This was, however, not immediately reflected in the results. As shown in Fig. 5,  $ZnO_{(d)}\%$  continued to drop as pH increasing from 6.9 to 9.9. In fact, the lowest  $ZnO_{(d)}\%$  was observed at pH = 9.9. These results suggest that the reactions in Eqs. (8) and (9) did not start immediately as pH increased to weak alkaline ( $pH \leq 9.9$ ). Instead, it is suspected that Eq. (10) might represent the predominant reaction at such pH levels with  $Zn(OH)_2$  being the main product on ZnO film surfaces. A previous study found that  $Zn(OH)_2$  had very low solubility in weak alkaline solution and only became soluble at pH = 11 or higher [30]. Due to its low solubility at such pH levels, the  $Zn(OH)_2$  layer may have protected the ZnO film from further dissolution and reaction with  $OH^-$ . The overall result is a low  $ZnO_{(d)}\%$ , as shown in Fig. 5. The significant increase of  $ZnO_{(d)}\%$  at pH = 10.9 indicates Eqs. (8) and (9) had started at this pH level, at which both ZnO and  $Zn(OH)_2$  became soluble by forming hydroxo complexes with  $OH^-$ .

A further study was conducted to provide further evidences to the discussions above. EDS was used to examine the surface composition of ZnO films after 3 h of exposure at the five pH levels between 4 and 12. As shown in Table 1, the Zn/O atom ratio on ZnO film surfaces was generally unchanged after exposure in acidic or weakly alkaline ( $pH = 8.1$ ) solution. Interestingly, a notable decrease in Zn/O ratio was observed at pH = 10.1, indicating an increasing amount of O relative to Zn atoms on ZnO surfaces. This is likely to be the result of the formation of  $Zn(OH)_2$ . At pH = 12.0 the Zn/O ratio reversed higher, as no residual  $Zn(OH)_2$  would be formed on ZnO surfaces because  $Zn(OH)_2$  is highly soluble at pH = 12 [30].

The results in our study may be related to the findings in earlier studies. Pardeshi and Patil [31] studied the influence of pH on ZnO photocatalyst and found that the degradation efficiency of phenol decreased by up to 17% and 35% in strong alkaline and acidic environment. The decreased efficiency in strong alkaline environment was ascribed to the negative charges on ZnO surfaces which presumably repelled away phenolate intermediates. Similar results were reported in another study by Lathasree et al. [25], where the decreased efficiency was ascribed to the zero point charge (zpc) of ZnO at 8.0. As our results have shown, it is likely that the ZnO photocatalysts in both studies had undertaken considerable dissolution

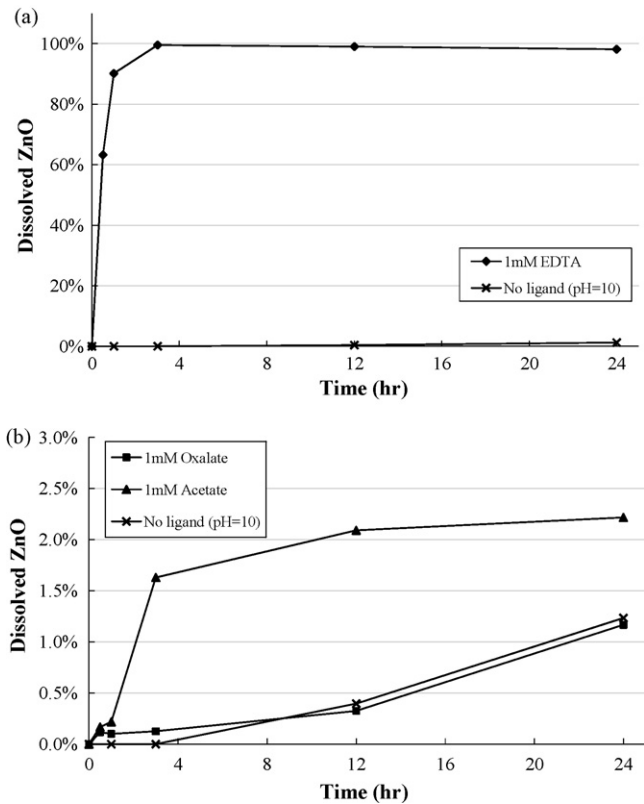


Fig. 6. Dissolution of ZnO films in 1 mM ligand solutions at pH = 10: (a) EDTA; (b) oxalate and acetate.

at extreme pH conditions, which would inevitably lead to activity deterioration of ZnO photocatalysts.

### 3.2.2. Dissolution in ligand solutions

Literature indicates that recent studies on ligand-induced dissolution of ZnO have been very limited. A study by Garcia Rodenas et al. [32] reported that ZnO particles with an average size of 300 nm suffered fast dissolution in the presence of oxalic acid at 70 °C. However, as the reaction was conducted at pH = 3.5, the sole effect of ligand (oxalate) remained unclear as our results showed that ZnO would rapidly dissolve in water at such pH.

EDTA, oxalic acid and acetic acid were selected to investigate their effects on ZnO dissolution. EDTA is a strong chelating agent that is widely used in the food industry as a stabiliser to prevent food spoilage and preserve food colour and flavour. It is also used in detergents to form soluble complexes with calcium and magnesium ions that are often present in hard water. In aqueous solutions, EDTA can form a complex with  $Zn^{2+}$  in a 1:1 EDTA-to-Zn ratio by forming two bonds with  $Zn^{2+}$ . The conjugate base of oxalic acid, oxalate, is also an excellent ligand which can react with metal ions and form a 5-membered  $MO_2C_2$  ring. Acetic acid is a common food ingredient and also a weak ligand. As a ligand it is used to produce de-icing salts, in which the effective compound is calcium magnesium acetate.

The results of ZnO dissolution in ligand solutions are shown in Fig. 6. To demonstrate the sole effect of ligand, the initial pH of each solution was adjusted to 10 to minimise the influence of pH. As shown in Fig. 6(a), ZnO film reacted rapidly with EDTA and dissolved completely after 3 h in 1 mM EDTA solution. On the contrary, only minimal dissolution (2.2%) was found in 1 mM acetate solution after 24 h. The presence of oxalate virtually had no noticeable acceleration effect on ZnO dissolution. A quick conclusion from Fig. 6 is that EDTA is highly corrosive to ZnO films while oxalate and acetate

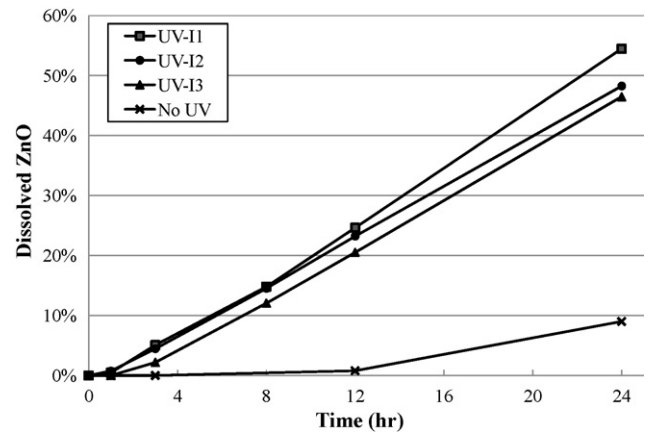


Fig. 7. Photo-dissolution of ZnO films under UV irradiation in 24 h ( $I_1 = 6.5 \text{ mW/cm}^2$ ,  $I_2 = 4.9 \text{ mW/cm}^2$ ,  $I_3 = 3.8 \text{ mW/cm}^2$ ).

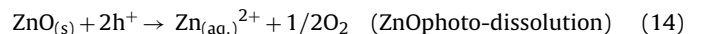
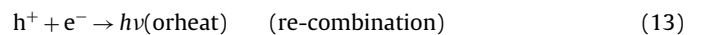
ions have minimal or negligible influence on ZnO dissolution. The reason for this, however, remains unclear at this point.

It has been reported that both oxalate and acetate ions could form complexes with  $Zn^{2+}$  cations. An early study reported that oxalate ions could form a  $K_2Zn(C_2O_4)_2 \cdot 7H_2O$  complex with  $Zn^{2+}$  in potassium oxalate solutions [33]. The existence of zinc acetate is also well documented [34–36]. The critical difference of ZnO dissolution may be caused by the different solubility of the Zn-ligand complexes. Zinc disodium EDTA is a soluble salt while the other two complexes (zinc oxalate and zinc acetate) are only sparingly soluble in water. In oxalate and acetate solutions, the dissolution equilibrium was reached after a small amount of zinc-ligand complexes was formed and dissolved in the solution. The very low yet slowly increasing  $ZnO_{(d)}$  in acetate solutions indicate that a layer of zinc acetate may have slowly formed on ZnO film surfaces, given the fact that there was no precipitate in the solution. This zinc acetate layer may have protected the inner ZnO film from further reaction and dissolution due to its low solubility in water.

### 3.3. Photo-dissolution and suppression effect

#### 3.3.1. Photo-dissolution

As shown in Fig. 7, the application of UV irradiation significantly accelerated the dissolution of ZnO. This “photo-dissolution effect” may be due to the fact that residual photo-generated holes on ZnO surfaces could attack the Zn–O bond and disassociate  $Zn^{2+}$  from ZnO surface. The following reactions are proposed:



where  $ZnO_{(s)}$  is a solid ZnO film,  $h\nu$  is a photon that reached ZnO surface,  $h^+$  and  $e^-$  are photo-generated hole and electron on the ZnO film surface, and  $Zn_{(aq.)}^{2+}$  is a  $Zn^{2+}$  in aqueous solution. The following reaction may also occur when ZnO film is exposed to UV in water:



As we know, the number of holes ( $h^+$ ) that can be generated on ZnO surface in a certain time is dependent on the number of photons ( $h\nu$ ) that reached ZnO surfaces (Eq. (12)), which is proportional to the incident UV intensity. As shown in Eq. (14), a decrease in the number of holes ( $h^+$ ) available at ZnO surfaces will lead to less  $ZnO_{(s)}$  transforming into  $Zn_{(aq.)}^{2+}$ . This was observed in Fig. 7 that a small decrease of the incident UV intensity resulted in a decrease of the ZnO dissolution rate.

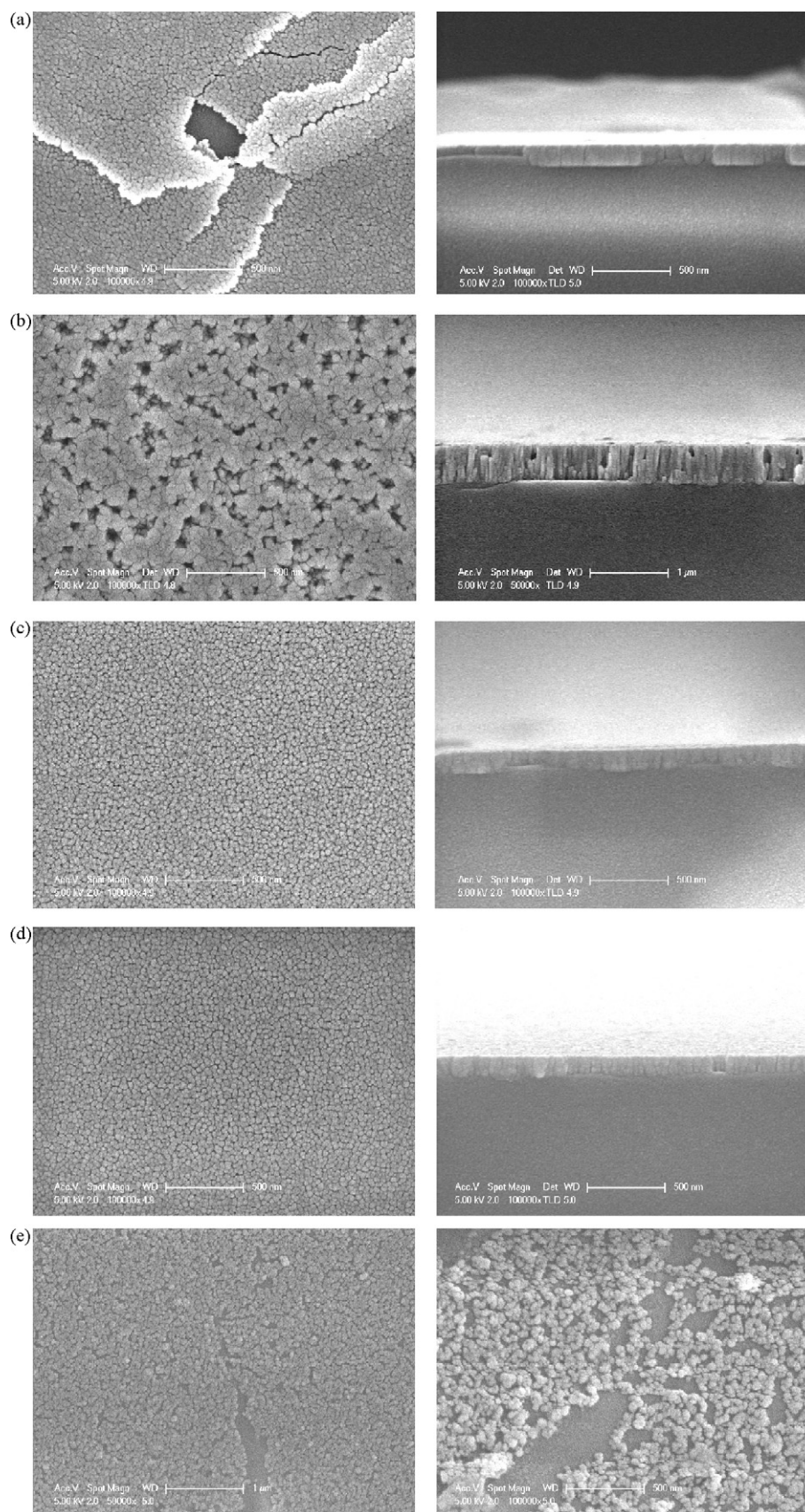


**Fig. 8.** SEM images of ZnO films after exposure under: (a) UV; (b) UV (500-nm-thick ZnO film); (c) pH=6; (d) pH=8; (e) pH=12.

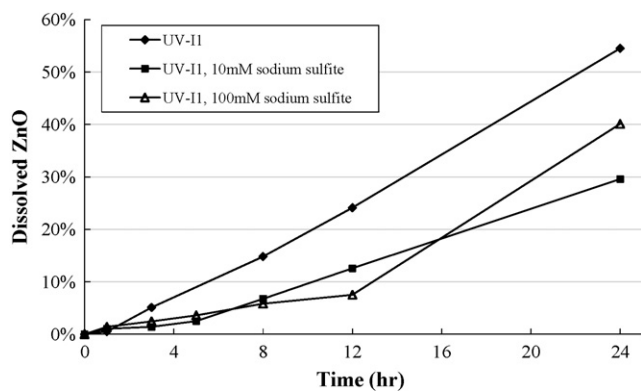


Fig. 9. Photo-dissolution of ZnO film in 10 mM and 100 mM  $\text{Na}_2\text{SO}_3$  solution in 24 h ( $I_1 = 6.5 \text{ mW/cm}^2$ ).

An early study noted that the photo-dissolution of ZnO under UV appeared to be 'pitting corrosion' [21]. As shown in Fig. 8(a), the ZnO film undertook localised dissolution on the surface under UV ( $I_1 = 6.5 \text{ mW/cm}^2$ ). It is suspected that the cracks appeared on the film were formed during sample preparation (rinsing and drying) due to the lack of strength of the corroded ZnO film. To further verify the results, this experiment was repeated using a thicker (500 nm) ZnO film which was exposed under UV for 3 h. The SEM images are shown in Fig. 8(b). No crack can be seen on the 500 nm ZnO film; however, many pits are shown on the film surface. The different surface morphology after the photo-dissolution may be caused by: (1) weaker mechanical strength of the 150 nm ZnO film during and after the photo-dissolution; (2) a monolayer of ZnO nanograins are present on the 150 nm ZnO film, while multiple layers of ZnO nanograins are present on the 500 nm ZnO film; (3) the nanograins of the 150 nm ZnO film appear to be smaller than those on the 500 nm ZnO film; (4) less time of UV exposure for the 500 nm film, i.e. 3 h vs. 6 h for 150 nm film. The localised photo-dissolution is different from the chemical dissolution of ZnO films in acid and alkaline solutions, in which the dissolution appeared to be uniform, as shown in Fig. 8(c), (d) and (e). This interesting phenomenon is related to the fact that holes and electrons are mostly generated from particular surface defect sites on nano-structured ZnO photocatalysts. The pitting dissolution of ZnO provides further evidence to Eq. (14) that photo-dissolution on ZnO films is caused by the attack of photo-generated holes.

### 3.3.2. Photo-dissolution with hole scavengers

The presence of hole scavengers was studied for its influence on ZnO photo-dissolution. The reason for this study is that most photocatalytic degradation reactions involve target compound(s) which may also act as hole scavengers. As shown in Eq. (15), it is possible that hole scavengers will compete with the reaction of ZnO photo-dissolution (Eq. (14)) by quickly consuming the holes generated in the photocatalysis process.

In this study,  $\text{Na}_2\text{SO}_3$  was used as hole scavengers and added in water to a concentration of 10 mM and 100 mM, respectively. The results are shown in Fig. 9. The result of ZnO photo-dissolution without hole scavengers is also shown in Fig. 9 for comparison. As expected, the presence of  $\text{SO}_3^{2-}$  considerably lowered the photo-dissolution rate of ZnO films, particularly in the first several hours. The 'route' of ZnO photo-dissolution was altered, with a two-stage process showing in both solutions. A distinct turning-point is shown at 12 h in the 100 mM  $\text{Na}_2\text{SO}_3$  solution, while a similar but less distinct turning-point can be seen at 5 h in the 10 mM  $\text{Na}_2\text{SO}_3$  solution. It is suspected that such turning-points are indications of complete consumption of  $\text{SO}_3^{2-}$  by photo-generated holes. As

$\text{SO}_4^{2-}$  could no longer act as hole scavengers, the rate of ZnO photo-dissolution accelerated from the turning-point in each solution.

## 4. Conclusions

In this study, potential dissolution and photo-dissolution of ZnO thin films (150 nm) were investigated under various corrosive environments. The results have shown that ZnO thin films suffered severe dissolution under: (a) extreme pH levels ( $\leq 5$  or  $\geq 11$ ); (b) 1 mM aqueous solution of EDTA; (c) UV ( $\lambda = 254 \text{ nm}$ ). The results are discussed in detail.

1. Between pH = 3 and 10, the dissolution rate of ZnO films showed an inverse dependence on pH. ZnO films suffered rapid dissolution in strongly acidic solutions (pH = 3–5). The slowest dissolution was observed at pH = 10, with 1.2% ZnO dissolved after 24 h. The trend quickly reversed at pH = 11, and the dissolution became rapid as pH increased to 12.
2. At all pH levels (3–12), ZnO thin films suffered severe dissolution after 1 week of exposure in water. The least dissolution of ZnO film (34%) was shown at pH = 10.
3. EDTA was highly corrosive to ZnO films. At pH = 10, the ZnO film completely dissolved within 3 h in 1 mM EDTA solution. Minimal dissolution was observed in 1 mM oxalate and acetate solutions after 24 h of exposure.
4. UV irradiation (254 nm) significantly accelerated the dissolution of ZnO films in water. A pitting corrosion effect was observed, with many pits shown on ZnO film surfaces after 24 h of UV exposure.
5. Hole scavengers ( $\text{Na}_2\text{SO}_3$ ) could compete with the photo-dissolution of ZnO films in water, resulting significant suppression on the photo-dissolution of ZnO films. This suppression effect remained until hole scavengers were completely consumed, from where the photo-dissolution accelerated.

Given the results in this study, it is concluded that considerations should be given in studies which involve the use of ZnO thin films as photocatalysts or self-cleaning materials in corrosive environments. Tests should be undertaken prior to exposing ZnO films in corrosive environments to avoid activity deterioration of ZnO photocatalysts or causing second pollution by free  $\text{Zn}^{2+}$  released from corroded ZnO films.

## Acknowledgements

The authors gratefully acknowledge the financial support of the Marsden Grant from the Royal Society of New Zealand. The authors would also like to thank Dr. Naresh Singhal and Dr. Yantao Song for their assistance in AAS measurements.

## References

- [1] S. Sakthivel, B. Neppolian, M.V. Shankar, B. Arabindoo, M. Palanichamy, V. Murugesan, Solar photocatalytic degradation of azo dye: comparison of photocatalytic efficiency of ZnO and  $\text{TiO}_2$ , Sol. Energy Mater. Sol. Cells 77 (2003) 65–82.
- [2] N. Gokon, N. Hasegawa, H. Kaneko, H. Aoki, Y. Tamaura, M. Kitamura, Photocatalytic effect of ZnO on carbon gasification with  $\text{CO}_2$  for high temperature solar thermochemistry, Sol. Energy Mater. Sol. Cells 80 (2003) 335–341.
- [3] A.J. Hoffmann, E.R. Carraway, M.R. Hoffmann,  $\text{TiO}_2$  photocatalytic oxidation mechanism of As(III), Environ. Sci. Technol. 22 (1988) 798–806.
- [4] L.C. Chen, Y.J. Tu, Y.S. Wang, R.S. Kan, C.M. Huang, Characterization and photoreactivity of N-, S-, and C-doped ZnO under UV and visible light illumination, J. Photochem. Photobiol. A 199 (2008) 170–178.
- [5] R. Georgekutty, M.K. Seery, S.C. Pillai, A highly efficient Ag-ZnO photocatalyst: synthesis, properties, and mechanism, J. Phys. Chem. C 112 (2008) 13563–13570.
- [6] R. Ullah, J. Dutta, Photocatalytic degradation of organic dyes with manganese-doped ZnO nanoparticles, J. Hazard. Mater. 156 (2008) 194–200.

- [7] S. Mozia, M. Tomaszewska, B. Kosowska, B. Grzmil, A.W. Morawski, K. Kalucki, Decomposition of nonionic surfactant on a nitrogen-doped photocatalyst under visible-light irradiation, *Appl. Catal. B* 55 (2005) 195–200.
- [8] H.F. Lin, S.C. Liao, S.W. Hung, The dc thermal plasma synthesis of ZnO nanoparticles for visible-light photocatalyst, *J. Photochem. Photobiol. A* 174 (2005) 82–87.
- [9] C.A.K. Gouvêa, F. Wypych, S.G. Moraes, N. Durán, N. Nagata, P. Peralta-Zamora, Semiconductor-assisted photocatalytic degradation of reactive dyes in aqueous solution, *Chemosphere* 40 (2000) 433–440.
- [10] S.K. Kansal, M. Singh, D. Sud, Studies on photodegradation of two commercial dyes in aqueous phase using different photocatalysts, *J. Hazard. Mater.* 141 (2007) 581–590.
- [11] N. Sobana, M. Swaminathan, The effect of operational parameters on the photocatalytic degradation of acid red 18 by ZnO, *Sep. Purif. Technol.* 56 (2007) 101–107.
- [12] X.J. Feng, L. Feng, M.H. Jin, J. Zhai, L. Jiang, D.B. Zhu, Reversible superhydrophobicity to super-hydrophilicity transition of aligned ZnO nanorod films, *J. Am. Chem. Soc.* 126 (2004) 62–63.
- [13] S.N. Das, J.H. Choi, J.P. Kar, J.M. Myoung, Tunable and reversible surface wettability transition of vertically aligned ZnO nanorod arrays, *Appl. Surf. Sci.* 255 (2009) 7319–7322.
- [14] D. Barreca, A. Gasparotto, C. Maccato, E. Tondello, U.L. Štangar, S.R. Patil, Photoinduced superhydrophilicity and photocatalytic properties of ZnO nanoplatelets, *Surf. Coat. Technol.* 203 (2009) 2041–2045.
- [15] J. Han, W. Gao, Surface wettability of nanostructured zinc oxide films, *J. Electron. Mater.* 38 (2009) 601–608.
- [16] StoCoat Lotusan™ Brochure, Sto Corporation, 2009. Website: <http://www.stocorp.com/allweb.nsf/lotusanpage>, at the time of writing (30 October 2009).
- [17] Pilkington Activ™ Global Brochure, Pilkington UK Ltd, November 2008. Website: <http://www.pilkington.com/resources/activglobalbrochure08i7002.pdf>, at the time of writing (30 October 2009).
- [18] Mills, A. Lepre, N. Elliott, S. Bhopal, I.P. Parkin, S.A. O'Neill, Characterisation of the photocatalyst Pilkington Activ™: a reference film photocatalysts, *J. Photochem. Photobiol. A* 160 (2003) 213–214.
- [19] M.V. Rao, K. Rajeshwar, V.R. Pal Verneker, J. DuBow, Photosynthetic production of H<sub>2</sub> and H<sub>2</sub>O<sub>2</sub> on semiconducting oxide grains in aqueous solutions, *J. Phys. Chem.* 84 (1980) 1987–1991.
- [20] Fruhwirth, G.W. Herzog, J. Poullos, Dark dissolution and photodissolution of ZnO, *Surf. Technol.* 24 (1985) 293–300.
- [21] P. Spathis, I. Poullos, The corrosion and photocorrosion of zinc and zinc oxide coatings, *Corros. Sci.* 37 (1995) 673–680.
- [22] M. Futsuhara, K. Yoshioka, Y. Ishida, O. Takai, K. Hashimoto, A. Fujishima, Micropattern formation on ZnO films using a photodissolution reaction, *J. Electrochem. Soc.* 143 (1996) 3743–3746.
- [23] H. Hidaka, Y. Suzuki, K. Nohara, S. Horikoshi, Y. Hisamatsu, E. Pelizzetti, N. Serpone, Photocatalyzed degradation of polymers in aqueous semiconductor suspensions. I. Photooxidation of solid particles of polyvinylchloride, *J. Polym. Sci. Part A: Polym. Chem.* 34 (1996) 1311–1316.
- [24] B. Neppolian, H.C. Choi, S. Sakthivel, B. Arabindoo, V. Murugesan, Solar/UV-induced photocatalytic degradation of three commercial textile dyes, *J. Hazard. Mater.* 89 (2002) 303–317.
- [25] S. Lathasree, A. Nageswara Rao, B. SivaSankar, V. Sadasivam, K. Rengaraj, Heterogeneous photocatalytic mineralisation of phenols in aqueous solutions, *J. Mol. Catal. A: Chem.* 223 (2004) 101–105.
- [26] E. Yassitepe, H.C. Yatmaz, C. Öztürk, K. Öztürk, C. Duran, Photocatalytic efficiency of ZnO plates in degradation of azo dye solutions, *J. Photochem. Photobiol. A* 198 (2008) 1–6.
- [27] J.C. Wang, P. Liu, S.M. Wang, W. Han, X.X. Wang, X.Z. Fu, Nanocrystalline zinc oxide in perfluorinated ionomer membranes: preparation, characterization, and photocatalytic properties, *J. Mol. Catal. A: Chem.* 273 (2007) 21–25.
- [28] D.G. Yoo, S.H. Nam, M.H. Kim, S.H. Jeong, H.G. Jee, H.J. Lee, N.E. Lee, B.Y. Hong, Y.J. Kim, D. Jung, J.H. Boo, Fabrication of the ZnO thin films using wet-chemical etching processes on application for organic light emitting diode (OLED) devices, *Surf. Coat. Technol.* 202 (2008) 5476–5479.
- [29] W. Stumm, J.J. Morgan, *Aquatic Chemistry: Chemical Equilibria and Rates in Natural Waters*, third ed., Wiley-Interscience, New York, 1996.
- [30] R.A. Reichle, K.G. McCurdy, L.G. Hepler, Zinc hydroxide: solubility product and hydroxy-complex stability constants from 12.5–75 °C, *Can. J. Chem.* 53 (1975) 3841–3845.
- [31] S.K. Pardeshi, A.B. Patil, A simple route for photocatalytic degradation of phenol in aqueous zinc oxide suspension using solar energy, *Sol. Energy* 80 (2008) 700–705.
- [32] L.A.G. Garcia Rodenas, M.A. Blesa, P.J. Morando, Reactivity of metal oxides: thermal and photochemical dissolution of MO and MFe<sub>2</sub>O<sub>4</sub> (M = Ni, Co, Zn), *J. Solid State Chem.* 181 (2008) 2350–2358.
- [33] V. Metler, The system zinc oxalate, potassium oxalate, water. II. At 35°, *J. Am. Chem. Soc.* 56 (1934) 1509–1510.
- [34] A.W. Davidson, W.H. McAllister, Solutions of salts in pure acetic acid. III. Zinc acetate and sodium zinc acetate, *J. Am. Chem. Soc.* 52 (1930) 519–527.
- [35] M. Pancholy, S.P. Singal, Ultrasonic studies in aqueous solutions of zinc acetate, *J. Phys. Soc. Jpn.* 17 (1962) 1657–1660.
- [36] G.C. Didonato, K.L. Busch, A reinvestigation of the mass-spectra of zinc acetate and cobalt acetate, *Inorg. Chem.* 25 (1986) 1551–1556.